Effect of Combination of Fly Ash and Bauxite Residue on the Fresh and Hardened States Properties of Cement Compositions

Luana Maria Vilaça da Silveira[1], Roberto Cesar de Oliveira Romano[2], Rafael Giuliano Pileggi[3] and Maria Alba Cincotto[4]
1. MSc candidate
2. Researcher
3. Professor
4. Professor
Polytechnic School of the University of São Paulo, São Paulo, Brazil
Corresponding author: luana.silveira@lme.pcc.usp.br

Abstract

The investigation of the use of bauxite residue from the Bayer process in association with Portland cement has grown substantially in recent years, but there are still uncertainties regarding aspects related to environmental issues and pathologies after the hardening of the cementitious component. The high alkali content and salinity, resulting from the bauxite digestion with NaOH, can leave free and soluble ions in the material, that if not fixed by association with cement, can culminate in efflorescence, leaching, and alkali-silica reaction. The positive effect of the addition of supplementary cementitious materials in cementitious products with the residue has already been observed, with improvement of some properties in the ternary system. In addition to technical issues, logistics must also be considered when choosing raw materials, as the high cost of long-distance transport can be an impediment to the large-scale use of the residue. Therefore, in this work fly ash generated in an alumina plant was chosen to combine with its bauxite residue in compositions formulated with Portland cement from the region, making the aspects related to the transport economically viable. This work aims to investigate the impact on the fresh and hardened state properties of pastes with different levels of additions. The results show that fly ash has a positive effect on pastes, resulting in better mechanical and microstructural properties of ternary systems in relation to the binary of cement with the residue. The addition of fly ash improves the flow of the pastes and delays the gain of consistency and agglomeration of particles. In this way, the combination of these materials can make the cementitious system more eco-efficient, durable and reduce environmental risk, allocating two industrial residues for large-scale application, in addition to reducing the consumption of cement in the compositions.

Keywords: Bauxite residue, Red mud, Fly ash, Synergistic effect, Ternary cementitious mixtures.

1. Introduction

Only about 3 % of the bauxite residue generated from the Bayer process (here called only as BR, to simplify) is successfully used on an industrial scale, most of which in civil construction [1]. According to the International Aluminum Institute [2], BR generation is equivalent to 4 % of cement production, and due to its chemical and mineralogical characteristics, has potential to be applied in association to the cement during the production of clinker Portland or in the compositions of cement components, contributing with the development of a large-scale application.

Several studies in recent years have shown the possibility of obtaining products suitable for use in civil construction, with improved microstructural, mechanical, and hygroscopic properties [3,4]. *Pontikes and Angelopoulos* [5] presented a review of some applications of bauxite residue in association with Portland cement, providing a critical point of view on the research conducted in the last 40 years, pointing out that the main barrier for the transition from the laboratory scale to the industry is the economic aspect. *Ribeiro, Labrincha and Morelli* [6] identified that the use of BR in cementitious compositions can be beneficial in the corrosion resistance of reinforcement concrete, due to its high alkalinity and presence of aluminosilicates. *Viyasun et al.* [7] observed an increase in compressive, tensile and bending strengths in compositions with 20 and 30 % replacement of cement by BR. *Romano et al.* [8], showed that bauxite residue can be used as an alkaline activator to ground blast furnace slag, producing compositions with zero-Portland cement. In chemical reaction, *Fujii et al.* [9] and *Romano et al.* [10] observed a delay in the cement reaction, with an increase in the induction and acceleration periods, reducing the formation of the main hydrated products and increasing the formation of ettringite. *Dodoo-Arhin et al.* [11] indicated that up to 5 % of substitution of Portland cement by the BR in compositions of pavements did not affect the mechanical strength or water absorption. *Romano et al*. [12] showed the impact of using BR in microconcrete of Portland cement and did a comparison with other kinds of ordinary supplementary cementitious materials, concluding that this practice is technically viable.

Consequently, the use of BR in this sector has the potential to contribute to reducing the energy spent in the related processes, the use of natural resources, the storage of BR and CO_2 emissions [2]. However, the use of BR in cementitious compositions is complex and many other characteristics still need to be investigated to scale-up its production. The high alkali content and the high salinity, resulting from the treatment of bauxite with NaOH, can leave free and soluble ions in the formed material. If they are not treated to try to mitigate these effects, fixing the free ions, pathological manifestations can occur in the materials in which the residue is reused, such as efflorescence, leaching and alkali-silica reaction (ASR) [13,14].

The addition of supplementary cementitious materials (SCM) in concrete mixtures is widely recognized as the most practical way to diminish ASR in cementitious compositions, acting as mitigating agent to sequester free ions [15]. The most used SCMs are limestone, ground granulated blast furnace slag and natural pozzolans. Fly ash (FA) can also be used as SCM, being collected from coal furnace filters of thermoelectric power plants, rich in reactive silica and alumina, containing little or no CaO. When combining SCM and/or inert material with Portland cement, it is possible to have a synergistic effect in the binary or ternary systems, with superposition of physical and chemical effects in the mixture, resulting in better mechanical and microstructural properties [16].

In addition to technical concerns after hardening of the cementitious component, logistical issues must also be considered when combining different raw materials. The high cost of transport over long distances can be an impediment to the large-scale use of the residue [1,2]. Thus, it is important to evaluate the use of BR in local synergies, making its transport economically viable.

This work aims to investigate the impact of the addition of BR and FA in cement pastes in the fresh and hardened states. Both additions combined are generated from the same alumina plant, in the northeast region of Brazil, and the cement is also from the same region. Isothermal conduction calorimetry in addition to rotational and oscillatory rheometry were used to analyze the fresh properties and the transition from fluid to solid state; and total porosity, splitting tensile strength and dynamic modulus of elasticity were employed for the hardened state evaluations at 28 days of curing.

2. Materials

The pastes were formulated with bauxite residue (BR) and fly-ash (FA) from the aluminum plant in São Luís, Maranhão, northeastern Brazil, dried at 105 °C for 24 h. The BR was ground and sieved through a 106 µm mesh opening and the FA was sieved through the same mesh. All tests presented here were made with the materials with this preparation. The cement was a Brazilian Portland cement named according to the national standard [17] as CPIV, commonly found in northeastern Brazil, with a specified composition of clinker and calcium sulfate, limestone filler up to 10 % and pozzolanic material from 15 % up to 50 %.

The physical characteristics of the materials are given in Table 1. Real density was determined in a gas He pycnometer, Micromeritics – AccuPyc II 1340. The specific surface area was determined in a Belsorp-Max – Bel Japan equipment according to the BET method, after sample treatment in a Belprep-vac II equipment at 40 °C and 10^{-2} kPa vacuum for 24 h. Particle size distributions, shown in Figure 1, were evaluated in a Helos – Sympatec laser granulometer, with a detection range of 0.1 – 350 micra, using deionized water as the dispersing medium.

Table 1. Physical characteristics of raw materials.

Characteristics	BR	FA	CPIV
Real density (g/cm^3)	3.12	2.43	2.93
Specific surface area (m^2/g)	17.8	13.9	1.97
d_{10} (µm)	0.94	7.02	2.80
d_{50} (µm)	4.73	34.81	17.0
d_{90} (µm)	16.8	83.7	49.5

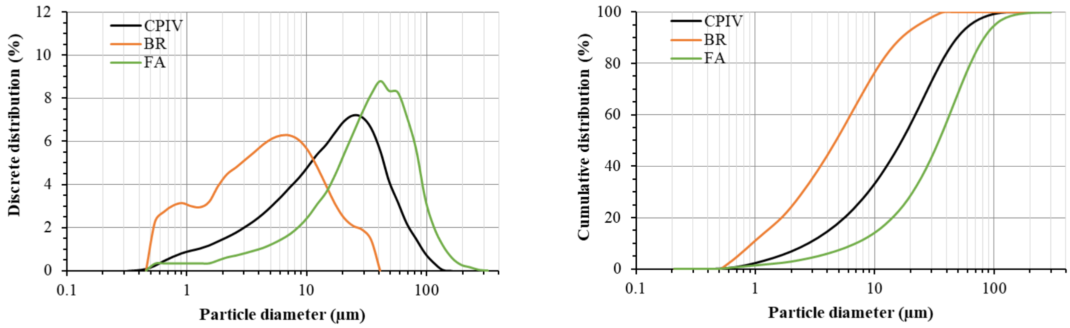

Figure 1. Laser granulometry particle size distribution of raw materials (discrete distribution on the left and cumulative distribution on the right).

The particle size distributions of the materials differ from each other and the finer granulometry of BR demonstrates its potential to act as a filler material, which can also improve the packing of cementitious pastes. The density of BR is close to that of cement, implying that its addition will not cause significant changes in the density of the composition. The same does not happen for FA. The specific surface areas of the additions are significantly larger than that of cement, which may imply a greater demand for water in these compositions to coat and distance particles to initiate the flow, affecting the rheological properties, reactivity, and hardened state of the formulated pastes. However, in this work the evaluations were performed fixing the water-to-solid content in order to have a fixed parameter to compare the compositions, and the changes on the fresh state properties were discussed.

Table 2 presents the chemical compositions determined by X-ray fluorescence (XRF) in a PANalytical spectrometer, Zetium model. CPIV presents conventional contents of their chemical species, with silica and calcium contents around 40 %. Concerning the BR, its iron, alumina, and sodium content are considerably higher, and FA has a considerable amount of silica.

The soluble ions in water were quantified by mixing 5 g of the material in 50 ml of deionized water, applying the recommendations of ASTM C114-18 [18] and the Brazilian standard NBR 13810 [19]. The BR has 0.16 % of Na_2O and < 0.01 % of K_2O and the FA has 0.12 % and 0.05 % of each oxide, respectively.

Table 2. Chemical compositions detected in raw materials (XRF – oxide compositions of dried material).

Constituents (wt. %)	BR	FA	CPIV
Loss on ignition (LOI)	14	15.9	4.42
SiO_2	12.2	37.2	38.3
CaO	2.55	12.5	40.3
MgO	0.18	1.00	1.09
Fe_2O_3	38.3	8.61	4.26
Al_2O_3	22.1	16.0	6.06
MnO	0.02	0.04	0.51
TiO_2	3.49	0.73	0.43
SO_3	-	5.19	3.27
Na_2O	5.82	0.89	0.28
K_2O	0.02	1.42	0.65
P_2O_5	0.06	0.13	0.13

The pozzolanic activity index was evaluated according to the Brazilian standard NBR 15895 [20], in order to determine the calcium consumption of each addition. It is important to emphasize that, by definition, a pozzolan is a siliceous or siliceous-aluminous material that contains an amorphous phase capable of reacting with lime in the presence of water, forming calcium silicate hydrate (C-S-H). In the case of BR, sodium aluminate reacts with $Ca(OH)_2$, precipitating calcium aluminate, not being classified as a pozzolan, in addition to the fact that it has crystalline and reactive phases. The BR has a consumption of 418 mg $Ca(OH)_2$/g of material and the FA 325 mg $Ca(OH)_2$/g of material.

The mineralogical compositions were determined by X-ray diffraction (XRD) in PANalytical diffractometer, Empyrean model. Tests were carried out with copper tube radiation, automatic gap of 0.5°, nickel filter and spinning frequency of 2 s per spin, step of 0.02°, staying at each step for 300 s, in the range of $5 < 2\theta < 70$. A qualitative analysis was carried out, not quantifying each phase with Rietveld analysis. Characteristic phases of a cement containing pozzolan (CPIV) were found, as well as calcite, gypsum and ettringite, illustrating a little pre-hydration of binder. In BR, hematite and goethite were identified, due to the marked presence of iron (more than 30 %), sodalite from the treatment of the ore with NaOH, and gibbsite, indicating the aluminum present in the bauxite mineral. The presence of a mineral with Ti was also found, anatase, and calcite. In FA, quartz, calcite, hematite, enstatite, mica, muscovite, gypsum, and wollastonite were identified, in addition to an amorphous halo, indicating a material without a defined crystalline structure.

Figure 2 shows the thermogravimetric analysis determined in a Netzsch thermobalance, T209 F1 model. The heating rate was maintained at 10 °C/min up to the temperature of 1000 °C, in an analytical N_2 atmosphere, flow of 20 ml/min, and the volatized gases purged at a rate of 10 ml/min.

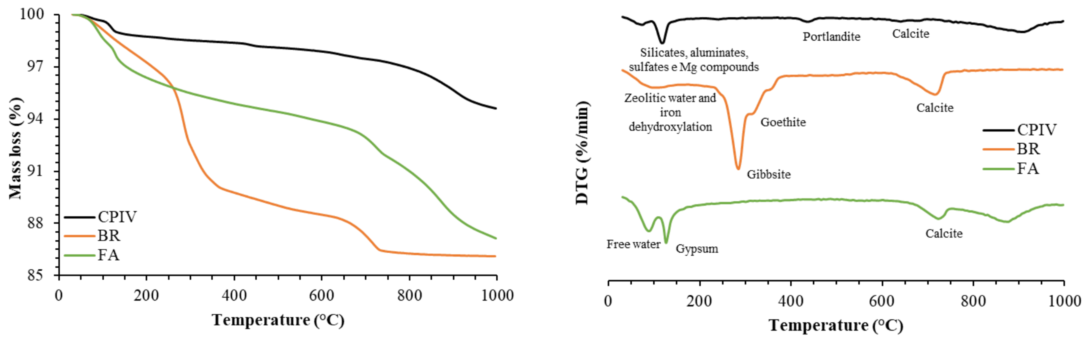

Figure 2. Thermogravimetric analysis of raw materials (mass loss on the left and its first derivative on the right).

The presence of portlandite ($Ca(OH)_2$) also indicates the pre-hydration of the cement, however with a low value, not being harmful to the results, which indicates that it may come from the material production process itself. The mass loss over the temperature of 600 °C is higher than the LOI shown in Table 2, indicating the presence of calcite in the cement. In BR, it is possible to see the peaks of the minerals gibbsite, goethite, and calcite, also found in the XRD results. In FA, gypsum and calcite were also identified.

3. Methods

The pastes were produced with different contents of BR and FA partially replacing the cement, ranging from 0 to 30 % by volume, and a fixed water/solid ratio of 0.5 wt., as shown in the mix design of Table 3.

Table 3. Mix design of the pastes.

Formulation ID	BR (g)	FA (g)	CPIV (g)	Replacement level of cement (% vol.)
100CPIV	*0*	*0*	*200*	*0*
90CPIV_10BR	21.2	0	178.8	10
80CPIV_20BR	42.1	0	157.9	20
70CPIV_30BR	62.7	0	137.3	30
90CPIV_10FA	0	16.9	183.1	10
80CPIV_20FA	0	34.4	165.7	20
70CPIV_30CV2	0	52.5	147.6	30
90CPIV_5BR_5FA	10.7	8.34	181.0	10
80CPIV_10BR_10FA	21.5	16.8	161.8	20
70CPIV_15BR_15FA	32.5	25.3	142.3	30

To mix the pastes, the powders were homogenized in a plastic container, and then water was added. A manual premix was carried out for 1 minute. Then, the container was placed in a Flacktek speed mixer equipment, where it was mixed for 2 minutes at a rotation speed of 1500/minute. For the hardened state properties, cylindrical molds 50 x 20 mm were casted, and the specimens were placed for curing in a dry chamber, inside a tray with a beaker filled with water, and sealed with a plastic bag for up to 28 days.

As the chemical reactions of Portland cement are a series of exothermic reactions, it can be monitored with isothermal conduction calorimetry. The main processes are well known, in which clinker phases hydrate in different kinetics, resulting mainly in the formation the hydrated products C-S-H, portlandite (CH), ettringite (Aft) and monossulfoaluminate (Afm). The quantification of the released heat flow was quantified in a Calmetrix I-CAL 8000 HPC isothermal conduction calorimeter, with a controlled temperature of 23 ºC for a period of 72 hours.

The free flow of the pastes was analyzed using a Kantro's mini-slump test. The paste was inserted in an acrylic cone of 6 cm high, smaller base of 2 cm and bigger base of 4 cm, placed on a glass base [21]. The paste was densified to avoid air bubbles, and the excess was removed from de top of the cone. The mold was rapidly lifted, and the spreading of each axis was recorded as the free flow, as an average of the four values.

The determination of the rheological parameters of the cementitious compositions was made by rotational and oscillatory rheometry, in a Mars 60 rheometer, Haake, using a parallel plate geometry of 35 mm of diameter, 1 mm gap and temperature control in 23 °C. For rotational rheometry, two shear cycles with linear control of rate variation were applied. During acceleration, it varied from 0 to 50 s^{-1}, with 10 points, and during deceleration, it returned from 45 s^{-1} to 0, with 9 points. For oscillatory rheometry, the time sweep procedure was used, performed with constant frequency at 1 Hz and strain also constant at 6.28 rad/s, for 5 hours.

For the hardened state properties at 28 days, the recommendations of the Brazilian technical standard NBR 7222 [22] were applied to obtain the mechanical strength, getting the splitting tensile strength, the guidelines of the Brazilian technical standard NBR 15630 [23] were used to calculate the dynamic modulus of elasticity, and the total porosity was obtained by the immersion test of Archimedes.

4. Results and Discussion

4.1 Fresh State Properties

The main stages of cement's chemical reactions are briefly explained below:

1. Initial dissolution, with wetting and neutralization of electrostatic charges: in its constitution, cement has mainly the phases tricalcium silicate/alite (C3S), dicalcium silicate/belite (C2S), tricalcium aluminate (C3A), brownmillerite (C4AF), calcium sulfate ($CaSO_4$) and free lime (CaO). With the wetting, ions SO_4^{2-}, Ca^{2+}, OH^-, K^+, Na^+, $[Al(OH)_4]^-$ and $H_2SiO_4^{2-}$ are released into the solution [24].

2. Induction period, with low dissolution rate and Ca^{2+} concentration below the limit of saturation: the grain's surface becomes wet and hydration products start to precipitate. C-S-H nucleates quickly, but in small amounts, as it needs time to build up and grow in proportional growth sites on the surface [25]. BR and FA could influence this stage, as they have a specific surface area larger than that of cement, being able to act as nucleation sites.

3. Acceleration period, accentuating the formation of C-S-H and CH: C-S-H and CH grow rapidly, through the following chemical equation (1) hydration of alite:

$$C3S + 5{,}3H_2O = xCaO.SiO_2.yH_2O + Ca(OH)_2 \quad (1)$$

   The 'x' and 'y' represent the variation on C-S-H structure, due to the cement composition, w/c ratio and hydration conditions, also forming a structure with chemical substituents, such as Al^{3+} and SO_4^{2-} [26], which could come from BR and FA.

4. Deceleration period, with depletion of sulfate forming Aft, and later transformation in Afm: sulfate has been consumed since the beginning of the reaction, but its depletion occurs after the acceleration period.C-S-H and CH continue to form, but more slowly, slowing down the overall reaction [4].

Table 4Table shows the results (normalized to cement content) of the main stages of reactions obtained by isothermal conduction calorimetry.

Table 4. Isothermal conduction calorimetry results.

Formulation	Total cumulative heat (J/g)	Duration of induction period (h:min)	Reaction rate at acceleration period (10^{-3} W/g.h)	Heat at second peak * (10^{-3} W/g)	Time at second peak * (h:min)	Heat at third peak ** (10^{-3} W/g)	Time at third peak ** (h:min)
100CPIV	*180.6*	*1:36*	*0.29*	*1.85*	*10:00*	*0.76*	*29:10*
90CPIV_10BR	205.8	1:24	0.31	1.98	8:50	1.51	20:50
80CPIV_20BR	240.1	1:12	0.42	2.18	8:20	2.26	17:00
70CPIV_30BR	257.2	1:12	0.53	2.38	7:35	2.93	14:00
90CPIV_10FA	184.6	1:03	0.30	1.71	8:00	0.83	26:10
80CPIV_20FA	203.0	0:45	0.32	1.90	6:25	1.11	21:10
70CPIV_30FA	231.6	0:27	0.37	2.15	5:30	1.53	17:20
90CPIV_5BR_5FA	198.2	1:09	0.38	1.85	8:20	1.23	23:00
80CPIV_10BR_10FA	228.1	1:03	0.47	2.00	7:30	1.77	19:00
70CPIV_15BR_15FA	251.6	0:51	0.53	2.13	6:25	2.31	15:20

** referred to the end of acceleration period*
*** referred to the reaction of ettringite formation*

The greater the content of additions, the shorter the induction period, and the greater the reaction rate. BR and FA alter the hydration kinetics, acting as nucleation points for crystals to grow, intensifying the reactions due to the higher specific surface area and alkalinity.

The second peak, referred to the end of acceleration period, forming C-S-H and CH, is also anticipated and intensified, as well as the third peak (formation of Aft). This also shows the relation with the filler effect promoted by the additions, i.e., the seeding effect of fillers, as well as the chemical influence. With high alumina contents coming from BR and FA, phases such as stratlingite may precipitate and can be intermixed with the hydrated product C-S-H, forming calcium aluminate silicate hydrate (C-A-S-H) [27]. Consequently, the pH of the medium rises, shifting the equilibrium and changing the precipitation of the products, accelerating the reactions promoted by the higher alkalinity.

It’s been reported in the literature [28] that the effect of FA in the early times of hydration is mainly due to its filer effect, and its chemical contribution starts when the medium has sufficient alkalinity for its dissolution, consuming CH by the pozzolanic reaction. The extra alkalinity provided by the BR accelerates this process.

As for the BR, its effect depends on the type (origin) and content of the residue and the type of cement used [29], as it can delay the induction and acceleration periods [4], have no impact on the induction period [24] or shorten the induction period and accelerate the hydration [30]. The residue is able to interact with cement, forming new hydration products with the incorporation of sodium and aluminium, changing the hydration kinetics [24,31].

The hardening of cement pastes occurs by coagulation/flocculation, in addition to hydration reactions, therefore by chemical and physical parameters [9]. The particle size, morphological distribution, crystallinity, and surface charge are characteristics that have a direct influence on the chemical reaction and agglomeration. Furthermore, the reactivity and solubility of each raw material will also influence the gain in consistency. Therefore, it is important to carry out a combined assessment of the chemical and physical parameters to obtain a better understanding of the cause-effect of hardening. Agglomeration kinetics and chemical reaction kinetics are phenomena that occur in parallel and are directly related [29].

Figure 3 shows the free flow of the pastes, where is very clear that the higher the replacement content of cement, the lower the flow, that is, lower is the workability of the pastes. The loss of flowability was also noticed by other works with BR and/or FA, attributed to the high fineness of the residues, and the possibility of solubilization of ions retained in the gel, such as sodium and iron [30,32–36]. It is also possible to see an improvement in the flow on ternary compositions with replacement levels of 20 % and 30 % of cement, demonstrating the synergistic benefits between the materials in fresh properties.

Figure 3. Free flow of paste's formulations.

As the water/solid ratio is constant, there is a tendency of affecting the rheological parameters. Their evaluation is fundamental for understanding the behavior of pastes in their different rheological moments required by cementitious compositions, such as mixing, transport, application, and finishing. From the rotational rheometry test, it is possible to obtain the yield stress and the apparent viscosity. Yield stress is the minimum stress required for the onset of flow, being quantified as the shear stress value at the lowest shear rate used during the deceleration step. Apparent viscosity is obtained at the maximum shear rate. No model was applied to calculate these parameters, as they can generate errors in the interpretation of results. Thus, it was decided to adopt the real data, as presented in [37].

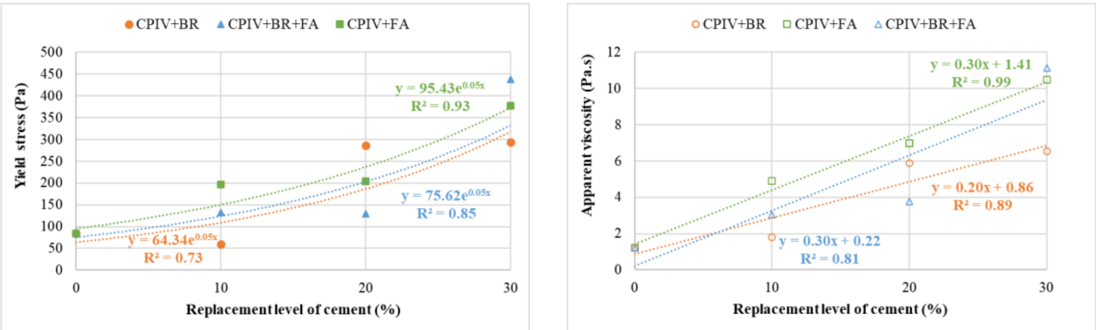

Figure 4. Yield stress (left) and the apparent viscosity (right) of each formulation.

Figure 4 shows the values of yield stress and apparent viscosity of each binary (CPIV+BR and CPIV+FA) and ternary (CPIV+BR+FA) systems.

The yield stress and the apparent viscosity increased with the increase of the mineral addition's contents, also seeing by [30]. In the case of pastes, where only small particles are present, the suspension is suffering superficial forces of attraction and repulsion and Brownian force, in addition to the hydrodynamic force generated by the flow under shear stress. There is a natural tendency for agglomeration due to the attraction between the charges of ions released into solution by raw materials. For there to be deagglomeration and flow, it is necessary that the repulsive forces dominate the attractive ones.

By incorporating BR and FA in the cementitious paste, which have higher specific surface area than cement, the agglomeration tendency is increased, due to the approximation of particles, increasing the collision between them and intensifying the ionic forces, which makes it difficult for the mixture to flow properly. The proper fluidity will happen when water fill the porosity of the system and keep the solid particles separated, avoiding the particles collision. The higher specific surface area of the additions requires more water to cover its particle's surface, reducing the free water to lubricate the solid particles. As a result, the internal friction of particles increase and the workability decreases [38].

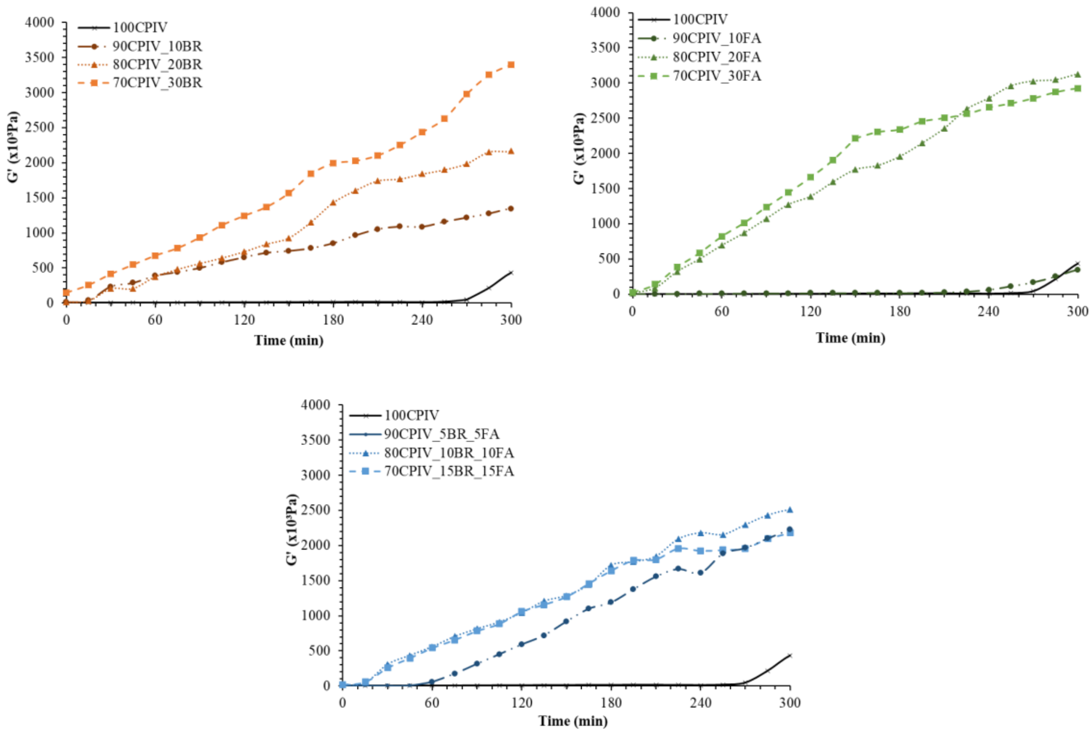

Figure 5. Evolution of G' over time of each formulation.

During the oscillatory rheometry test, applying a constant strain and frequency within the linear viscoelastic region, it is possible to monitor the changes in the viscoelasticity over time without breaking the microstructure. This change is correlated with the consistency gain over time, and it is represented by the storage modulus (G'), which expresses the elastic response of the material during the transition from fluid to elastic behavior during the hardening. Figure 5 shows the evolution of G' over time of each formulation, where the binary systems are shown above (CPIV+BR on the left and CPIV+FA on the right) and the ternary (CPIV+BR+FA) below.

The intensification of G' in the reference composition (100CPIV) starts at 4h15min, indicating an increase in particle agglomeration forces. The composition 90CPIV_10FA has a similar behavior, but with consistency gain occurring a little earlier, at 3h45min, and more slowly, with a lower stiffening rate, characterized by a smaller slope on the graphic. Therefore, it can be said that the addition of 10 % fly ash did not change considerably the consolidation of the paste.

The same does not occur for the other compositions with additions, in which it is possible to observe a different behavior from the reference sample, with an increase in consistency since the early ages of hardening. In addition, as the replacement content of cement increases, the consistency gain is more accentuated, represented by the increase in the slope of the line (rigidification rate). This happens due to increases in the specific surface area and surface charge of the particles, resulting in approximation and intensification of the agglomeration forces, and coagulation and flocculation over the time. In this way, the average distance between the particles and their mobility are reduced and the tendency to agglomeration is increased. With the intensification of chemical reactions and formation of hydrated products, these agglomerates become stable, and the bond strength was intensified [39,40].

4.2 Hardened State Properties

The results of total porosity, splitting tensile strength and dynamic modulus of elasticity of each formulation at 28 days are shown in Figure 6. The values of the reference composition (100CPIV) are shown as a dashed line on the graphs.

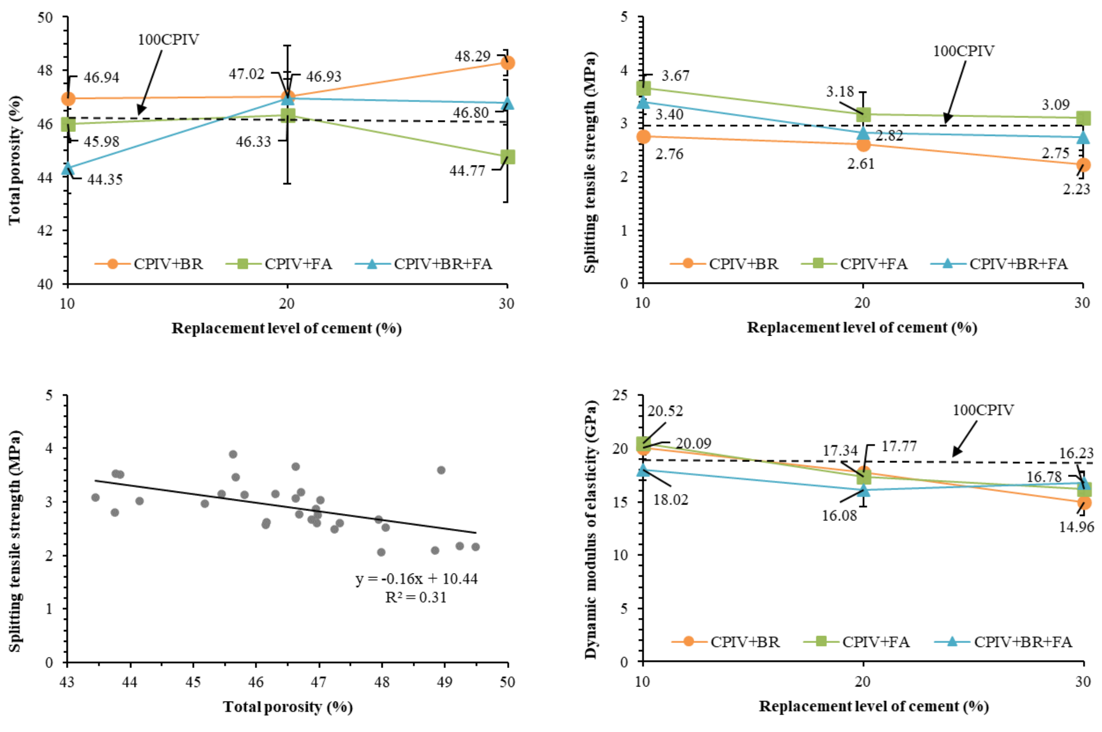

Figure 6. Total porosity, splitting tensile strength and dynamic modulus of elasticity of each formulation at 28 days.

The addition of BR can increase the total porosity of the composition. Despite the fineness of BR, which could fill in the pores of the material, the changes in the hydrated products can deteriorate the pore structure, coarsening it [30,38]. The addition of FA reduced the total porosity of the compositions and could improve this property in the ternary system. The addition of fine particles of FA causes segmentation of large pores, increases nucleation sites for precipitation of hydration products, and consumes CH, resulting in pore refinement [41]. The inclusion of materials with different specific surface areas and particle sizes distributions enabled the formation of a more compact matrix when more cement was replaced, filling voids and reducing the pores.

To assess the significance of the variation in the additions contents used, a statistical analysis One-way Anova was performed to accept or reject the hypothesis of equality of means, and the Tukey test to verify whether there was a statistical difference between samples with respect to properties in the hardened state of each system individually (CPIV+BR, CPIV+FA and CPIV+BR+FA). For total porosity, the statistical analysis for the system CPIV+BR is shown in Table 5 as an example.

Table 5. Statistical analysis for the system CPIV+BR.

SUMMARY

Group	*Count*	*Sum*	*Average*	*Variance*
100CPIV	3	138.48	46.16	0.72
90CPIV_10BR	3	140.82	46.94	0.00
80CPIV_20BR	3	141.06	47.02	0.81
70CPIV_30BR	3	144.88	48.29	0.23

ANOVA

Source of variation	*SQ*	*gl*	*MQ*	*F*	*P-value*	*F critical*
Between groups	7.02	3	2.34	**5.32**	0.03	**4.07**
Within groups	3.52	8	0.44			
Total	10.54	11				

TUKEY’S TEST

Compositions	100CPIV	90CPIV_10BR	80CPIV_20BR	70CPIV_30BR
100CPIV		0.515	0.437	0.018
90CPIV_10BR	2.028		0.999	0.135
80CPIV_20BR	2.242	0.214		0.166
70CPIV_30BR	5.562	3.534	3.320	

The “summary” presents the values of porosity of the specimens, the “Anova” indicates whether the hypothesis of equality between the results should be accepted or rejected (if F > F critical, and P-value < 0.05, then there is significance), and the “Tukey’s test” compares the variables ‘two-by-two’, meaning that when the cell is colored, its value is different from the group showed in the first column on the left. The results show that there are significant changes on the total porosity of 70CPIV_30BR and the reference composition (100CPIV). For the other systems (CPIV+FA and CPIV+BR+FA) it was also confirmed by Anova that there were changes in the porosity promoted by the use of additions, and the application of Tukey’s test, shown in Table 6, pointed out which compositions were different.

In case of splitting tensile strength, there is a tendency of decreasing this property with the increase in the replacement level of cement, because there is low amount of cement to guarantee the resistance. This was observed for every system (binary or ternary).

The third graph in Figure 6 shows a correlation between the total porosity and the splitting tensile strength, demonstrating that the higher the total porosity, the lower the mechanical strength. When compositions are produced using the same raw materials and proportioning, the mechanical strength and modulus of elasticity have a great correlation with total porosity. However, in this work, as different contents and types of mineral additions were used, the R^2 was lower than expected.

Table 6. Total porosity's Tukey's test for the systems CPIV+FA and CPIV+BR+FA.

SYSTEM CPIV+FA

Compositions	100CPIV	90CPIV_10FA	80CPIV_20FA	70CPIV_30FA
100CPIV		0.999	0.999	0.733
90CPIV_10FA	0.194		0.993	0.805
80CPIV_20FA	0.178	0.372		0.663
70CPIV_30FA	1.470	1.275	1.648	

SYSTEM CPIV+BR+FA

Compositions	100CPIV	90CPIV_5BR_ 5FA	80CPIV_10BR _10FA	70CPIV_15BR _15FA
100CPIV		0.115	0.690	0.796
90CPIV_5BR_5FA	3.692		0.024	0.032
80CPIV_10BR_10FA	1.579	5.271		0.997
70CPIV_15BR_15FA	1.299	4.991	0.280	

The statistical analysis of splitting tensile strength shows significance only for the systems CPIV+BR and CPIV +FA, whose Tukey's tests are shown in Table 7.

Table 7. Splitting tensile strength's Tukey's test for the systems CPIV+BR and CPIV+FA.

SYSTEM CPIV+BR

Compositions	100CPIV	90CPIV_10BR	80CPIV_20BR	70CPIV_30BR
100CPIV		0.588	0.140	0.003
90CPIV_10BR	1.838		0.659	0.015
80CPIV_20BR	3.496	1.659		0.073
70CPIV_30BR	7.641	5.803	4.145	

SYSTEM CPIV+FA

Compositions	100CPIV	90CPIV_10FA	80CPIV_20FA	70CPIV_30FA
100CPIV		0.024	0.625	0.844
90CPIV_10FA	5.264		0.137	0.076
80CPIV_20FA	1.744	3.520		0.975
70CPIV_30FA	1.158	4.105	0.585	

Therefore, comparing with the reference suspension, it can be said that:

- the addition of greater quantities of the BR reduces the mechanical strength of cementitious compositions;
- the addition of FA improves the mechanical strength in minor quantities (up to 10 %) and don't alter this property in greater amounts;
- the combination of FA and BR has a positive effect on cementitious compositions, improving the mechanical strength of ternary systems in relation to the binary of cement and BR, but still lower than using FA on the binary systems. In this case, replacement of 10 % resulted in mechanical performance of around 25 % higher than for the reference, but did not impact in changes statistically significant for replacements higher than 20 %.

For the dynamic modulus of elasticity, statistically relevant changes were observed for all the systems, whose Tukey's tests are shown in Table 8 For the system CPIV+BR, the replacement level of 30 % resulted in a product with lower modulus of elasticity comparing to all the others. For the binary system with FA, the higher replacement level had different rigidity from the reference and 10 % of addition. And as for the ternary system, only 80CPIV_10BR_10FA was different from the reference.

Table 8. Dynamic modulus of elasticity's Tukey's test for the systems CPIV+BR and CPIV+FA.

SYSTEM CPIV+BR

Compositions	100CPIV	90CPIV_10BR	80CPIV_20BR	70CPIV_30BR
100CPIV		0.346	0.269	0.001
90CPIV_10BR	2.525		0.023	0.000
80CPIV_20BR	2.809	5.334		0.008
70CPIV_30BR	9.263	11.790	6.454	

SYSTEM CPIV+FA

Compositions	100CPIV	90CPIV_10FA	80CPIV_20FA	70CPIV_30FA
100CPIV		0.258	0.213	0.028
90CPIV_10FA	2.854		0.013	0.002
80CPIV_20FA	3.062	5.916		0.500
70CPIV_30FA	5.129	7.983	2.067	

SYSTEM CPIV+BR+FA

Compositions	100CPIV	90CPIV_5BR_5FA	80CPIV_10BR_10FA	70CPIV_15BR_15FA
100CPIV		0.650	0.030	0.099
90CPIV_5BR_5FA	1.683		0.157	0.466
80CPIV_10BR_10FA	5.063	3.380		0.824
70CPIV_15BR_15FA	3.843	2.160	1.220	

5. Conclusion

This paper evaluated the effect on the fresh and hardened states properties of cement compositions made with fly ash and bauxite residue, to find out if they have a synergistic effect, improving the properties of the formed materials.

It was shown that both additions alter the hydration kinetics of cement pastes, acting as nucleation points for crystals to grow because of its higher specific surface area and alkalinity, intensifying the reactions and formation of hydration products. Although it has not been presented in this work, it is reported in the literature that FA intensifies the consumption of CH at advanced hydration times [28] and, in the case of BR, the impact will depend on the type and amount of residue used, which alter the hydration kinetics in different ways. In this work, the presence of the additions shortened the induction period, and accelerated and intensified the formation of the hydrated products.

The higher specific surface area of BR and FA and its chemical aspects, led to a tendency of agglomeration, due to the increased collision between the particles and intensification of ionic forces. Consequently, the yield stress and apparent viscosity increased with the increase of the addition's contents, making it difficult for the mixture to flow properly. Despite that, it was possible to see an improvement in the flow on ternary compositions with replacement levels of 20 % and 30 % of cement, demonstrating the synergistic benefits between the materials.

During the transition from fluid to elastic behavior in consolidation, the addition of 10 % FA did not change the hardening in relation to the reference sample (100 % cement). On the other hand, for the other formulations, the consistency increased right in the first moments of hydration, and, as the replacement content of cement increased, the consistency gain was more accentuated. This effect is also due to the increase in the specific surface area and surface charge of the particles, resulting in approximation and intensification of the agglomeration forces. In this way, the average distance between the particles and their mobility are reduced and the tendency of agglomeration is increased. As the BR has more fine particles than the cement, while the FA has coarser, the first dominated the effects in the ternary systems.

For the hardened state properties, there was a tendency of decreasing the splitting tensile strength and modulus of elasticity with the increase in the replacement level of cement. The combination of FA had a positive effect on cementitious compositions, improving the mechanical strength and reducing the total porosity of the compositions of ternary systems in relation to the binary of cement and BR.

The inclusion of materials with different specific surface areas and particle sizes, enabled the formation of a more packed matrix when more cement was replaced, resulting in better mechanical and microstructural properties. Therefore, when FA was added to the system with BR and CPIV, the different granulometry enable a pore refinement in the matrix, improving the properties, as the voids were better filled and reduced.

6. References

[1] K. Evans, The History, Challenges, and New Developments in the Management and Use of Bauxite Residue, J. Sustain. Metall. 2 (2016) 316–331. https://doi.org/10.1007/s40831-016-0060-x.

[2] IAI, Technology Roadmap: Maximising the use of bauxite residue in cement, International Aluminium Institute, 2020.

[3] E.P. Manfroi, M. Cheriaf, J.C. Rocha, Microstructure, mineralogy and environmental evaluation of cementitious composites produced with red mud waste, Construction and Building Materials. 67 (2014) 29–36. https://doi.org/10.1016/j.conbuildmat.2013.10.031.

[4] R.C.O. Romano, A.L. Fujii, R.B. Souza, M.S. Takeashi, R.G. Pileggi, M.A. Cincotto, Acompanhamento da hidratação de cimento Portland simples com resíduo de bauxita, Cerâmica. 62 (2016) 215–223. https://doi.org/10.1590/0366-69132016623632039.

[5] Y. Pontikes, G.N. Angelopoulos, Bauxite residue in cement and cementitious applications: Current status and a possible way forward, Resources, Conservation and Recycling. 73 (2013) 53–63. https://doi.org/10.1016/j.resconrec.2013.01.005.

[6] D.V. Ribeiro, J.A. Labrincha, M.R. Morelli, Effect of the addition of red mud on the corrosion parameters of reinforced concrete, Cement and Concrete Research. 42 (2012) 124–133. https://doi.org/10.1016/j.cemconres.2011.09.002.

[7] K. Viyasun, R. Anuradha, K. Thangapandi, D. Santhosh Kumar, A. Sivakrishna, R. Gobinath, Investigation on performance of red mud based concrete, Materials Today: Proceedings. 39 (2021) 796–799. https://doi.org/10.1016/j.matpr.2020.09.637.

[8] R.C.O. Romano, H.M. Bernardo, J.A.F.S. Mesquita, D.A. Niza, M.A. Cincotto, R.G. Pileggi, Evaluation of the hardened state properties of zero-cement mortars produced using bauxite residue as an activator to ground blast furnace slag, in: KU Leuven, Athens, 2018: pp. 293–300.

[9] A.L. Fujii, D. dos Reis Torres, R.C. de Oliveira Romano, M.A. Cincotto, R.G. Pileggi, Impact of superplasticizer on the hardening of slag Portland cement blended with red mud, Construction and Building Materials. 101 (2015) 432–439. https://doi.org/10.1016/j.conbuildmat.2015.10.057.

[10] R. Romano, H. Montefusco, M. Hark Maciel, R. Pileggi, M. Cincotto, Using isothermal calorimetry, X-ray diffraction, thermogravimetry and FTIR to monitor the hydration reaction of Portland cements associated with red mud as a supplementary material, Journal of Thermal Analysis and Calorimetry. (2019). https://doi.org/10.1007/s10973-019-08095-x.

[11] D. Dodoo-Arhin, R.A. Nuamah, B. Agyei-Tuffour, D.O. Obada, A. Yaya, Awaso bauxite red mud-cement based composites: Characterisation for pavement applications, Case

Studies in Construction Materials. 7 (2017) 45–55. https://doi.org/10.1016/j.cscm.2017.05.003.

[12] R.C. de O. Romano, J.A.F.S. Mesquita, H.B. Montefusco, G.P. Brasileiro, G.H.U. Muniz, M.A. Cincotto, R.G. Pileggi, Impact of Using Bauxite Residue in Microconcrete and Comparison with Other Kind of Supplementary Cementitious Material, in: 35th Conference and Exhibition ICSOBA, Hamburgo, 2017: pp. 505–518.

[13] C.C. Liberato, R.C. de O. Romano, M. Montini, J.B. Gallo, D. Gouvea, R.G. Pileggi, Efeito da calcinação do resíduo de bauxita nas características reológicas e no estado endurecido de suspensões com cimento Portland, Ambient. constr. 12 (2012) 53–61. https://doi.org/10.1590/S1678-86212012000400005.

[14] S.-P. Kang, S.-J. Kwon, Effects of red mud and Alkali-Activated Slag Cement on efflorescence in cement mortar, Construction and Building Materials. 133 (2017) 459–467. https://doi.org/10.1016/j.conbuildmat.2016.12.123.

[15] M.J. Tapas, L. Sofia, K. Vessalas, P. Thomas, V. Sirivivatnanon, K. Scrivener, Efficacy of SCMs to mitigate ASR in systems with higher alkali contents assessed by pore solution method, Cement and Concrete Research. 142 (2021) 106353. https://doi.org/10.1016/j.cemconres.2021.106353.

[16] C.S. Feltrin, G.C. Isaia, A. Lübeck, Synergic effects between mineral admixtures on strength and microstructure of concretes, Rev. IBRACON Estrut. Mater. 13 (2020) e13604. https://doi.org/10.1590/s1983-41952020000600004.

[17] ASSOCIAÇÃO BRASILEIRA DE NORMAS TÉCNICAS, NBR 16697 – Cimento Portland – Requisitos, (2018).

[18] ASTM International, ASTM C114-18 – Standard Test Method for Chemical Analysis of Hidraulic Cement, (2018).

[19] ASSOCIAÇÃO BRASILEIRA DE NORMAS TÉCNICAS, NBR 13810 – Água – Determinação de metais – Método de espectrometria de absorção atômica por chama, (1997).

[20] ASSOCIAÇÃO BRASILEIRA DE NORMAS TÉCNICAS, NBR 15895 – Materiais pozolânicos – Determinação do teor de hidróxido de cálcio fixado – Método Chapelle modificado, (2010).

[21] J.S. Raucci, R.T. Cecel, R.C.O. Romano, R.G. Pileggi, V.M. John, Effect of mixing method on the mini-slump spread of Portland cement pastes, Rev. IBRACON Estrut. Mater. 11 (2018) 410–431. https://doi.org/10.1590/s1983-41952018000200010.

[22] ASSOCIAÇÃO BRASILEIRA DE NORMAS TÉCNICAS, NBR 7222 – Concreto e argamassa – Determinação da resistência à tração por compressão diametral de corpos de prova cilíndricos, (2011).

[23] ASSOCIAÇÃO BRASILEIRA DE NORMAS TÉCNICAS, NBR 15630 – Argamassa para assentamento e revestimento de paredes e tetos – Determinação do módulo de elasticidade dinâmico através da propagação da onda ultrassônica, (2008).

[24] R.C.O. Romano, H.M. Bernardo, M.H. Maciel, R.G. Pileggi, M.A. Cincotto, Hydration of Portland cement with red mud as mineral addition, J Therm Anal Calorim. 131 (2018) 2477–2490. https://doi.org/10.1007/s10973-017-6794-2.

[25] K.L. Scrivener, P. Juilland, P.J.M. Monteiro, Advances in understanding hydration of Portland cement, Cement and Concrete Research. 78 (2015) 38–56. https://doi.org/10.1016/j.cemconres.2015.05.025.

[26] S. Goñi, F. Puertas, M.S. Hernández, M. Palacios, A. Guerrero, J.S. Dolado, B. Zanga, F. Baroni, Quantitative study of hydration of C3S and C2S by thermal analysis: Evolution and composition of C–S–H gels formed, J Therm Anal Calorim. 102 (2010) 965–973. https://doi.org/10.1007/s10973-010-0816-7.

[27] B. Lothenbach, K. Scrivener, R.D. Hooton, Supplementary cementitious materials, Cement and Concrete Research. 41 (2011) 1244–1256. https://doi.org/10.1016/j.cemconres.2010.12.001.

[28] F. Deschner, F. Winnefeld, B. Lothenbach, S. Seufert, P. Schwesig, S. Dittrich, F. Goetz-Neunhoeffer, J. Neubauer, Hydration of Portland cement with high replacement by siliceous fly ash, Cement and Concrete Research. 42 (2012) 1389–1400. https://doi.org/10.1016/j.cemconres.2012.06.009.
[29] R.C. de O. Romano, J.A.F.S. de Mesquita, H.M. Bernardo, D.A. Niza, M.H. Maciel, M.A. Cincotto, R.G. Pileggi, Combined evaluation of oscillatory rheometry and isothermal calorimetry for the monitoring of hardening stage of Portland cement compositions blended with bauxite residue from Bayer process generated in different sites in Brazil, Rev. IBRACON Estrut. Mater. 14 (2021) e14211. https://doi.org/10.1590/s1983-41952021000200011.
[30] D. Hou, D. Wu, X. Wang, S. Gao, R. Yu, M. Li, P. Wang, Y. Wang, Sustainable use of red mud in ultra-high performance concrete (UHPC): Design and performance evaluation, Cement and Concrete Composites. 115 (2021) 103862. https://doi.org/10.1016/j.cemconcomp.2020.103862.
[31] Using isothermal calorimetry, X-ray diffraction, thermogravimetry and FTIR to monitor the hydration reaction of Portland cements associated with red mud as a supplementary material, (n.d.) 14.
[32] M. Ghalehnovi, E. Asadi Shamsabadi, A. Khodabakhshian, F. Sourmeh, J. de Brito, Self-compacting architectural concrete production using red mud, Construction and Building Materials. 226 (2019) 418–427. https://doi.org/10.1016/j.conbuildmat.2019.07.248.
[33] R.-X. Liu, C.-S. Poon, Utilization of red mud derived from bauxite in self-compacting concrete, Journal of Cleaner Production. 112 (2016) 384–391. https://doi.org/10.1016/j.jclepro.2015.09.049.
[34] W.C. Tang, Z. Wang, Y. Liu, H.Z. Cui, Influence of red mud on fresh and hardened properties of self-compacting concrete, Construction and Building Materials. 178 (2018) 288–300. https://doi.org/10.1016/j.conbuildmat.2018.05.171.
[35] W.C. Tang, Z. Wang, S.W. Donne, M. Forghani, Y. Liu, Influence of red mud on mechanical and durability performance of self-compacting concrete, Journal of Hazardous Materials. 379 (2019) 120802. https://doi.org/10.1016/j.jhazmat.2019.120802.
[36] Y. Yao, Y. Li, X. Liu, S. Jiang, C. Feng, E. Rafanan, Characterization on a cementitious material composed of red mud and coal industry byproducts, Construction and Building Materials. 47 (2013) 496–501. https://doi.org/10.1016/j.conbuildmat.2013.05.030.
[37] R.C.O. Romano, R.G. Pileggi, Use of rheological models for the evaluation of cement pastes with airentraining agent in different temperatures, in: Nordic Rheology Society, Copenhagen, n.d.
[38] L. Senff, D. Hotza, J.A. Labrincha, Effect of red mud addition on the rheological behaviour and on hardened state characteristics of cement mortars, Construction and Building Materials. 25 (2011) 163–170. https://doi.org/10.1016/j.conbuildmat.2010.06.043.
[39] R. Romano, C. Liberato, M. Montini, J. Gallo, M. Cincotto, R. Pileggi, Evaluation of transition from fluid to elastic solid of cementitious pastes with bauxite residue using oscillation rheometry and isothermal calorimetry, Applied Rheology. 23 (2013). https://doi.org/10.3933/ApplRheol-23-23830.
[40] P.F.G. Banfill, RHEOLOGY OF FRESH CEMENT AND CONCRETE, (n.d.) 70.
[41] P. Chindaprasirt, S. Rukzon, Strength, porosity and corrosion resistance of ternary blend Portland cement, rice husk ash and fly ash mortar, Construction and Building Materials. 22 (2008) 1601–1606. https://doi.org/10.1016/j.conbuildmat.2007.06.010.